Theory of the Little-Parks effect in spin-triplet superconductors

Chengyun Hua [1,*] Eugene Dumitrescu [2] and Gábor B. Halász [1,†]

[1]*Materials Science and Technology Division, Oak Ridge National Laboratory, Oak Ridge, Tennessee 37831, USA*
[2]*Computational Sciences and Engineering Division, Oak Ridge National Laboratory, Oak Ridge, Tennessee 37831, USA*

The celebrated Little-Parks effect in mesoscopic superconducting rings has recently gained great attention due to its potential to probe half-quantum vortices in spin-triplet superconductors. However, despite the large number of works reporting anomalous Little-Parks measurements attributed to unconventional superconductivity, the general signatures of spin-triplet pairing in the Little-Parks effect have been less systematically investigated. Here we use Ginzburg-Landau theory to study the Little-Parks effect in a spin-triplet superconducting ring that supports half-quantum vortices; we calculate the field-induced Little-Parks oscillations of both the critical temperature itself and the residual resistance resulting from thermal vortex tunneling below the critical temperature. We observe two separate critical temperatures with a single-spin superconducting state in between and find that due to the existence of half-quantum vortices, each minimum in the upper critical temperature splits into two minima for the lower critical temperature. From a rigorous calculation of the residual resistance, we confirm that these two minima in the lower critical temperature translate into two maxima in the residual resistance below and establish the general conditions under which the two maxima can be practically resolved. In particular, we identify a fundamental trade-off between sharpening each maximum and keeping the overall magnitude of the resistance large. Our results will guide experimental efforts in designing mesoscopic ring geometries for probing half-quantum vortices in spin-triplet candidate materials on the device scale.

I. INTRODUCTION

Topological quantum computation based on Majorana bound states is a leading candidate for processing quantum information [1]. The vortex cores of topological superconductors, such as gapped p-wave superconductors, host such self-conjugate Majorana bound states at zero energy [2–4]. The search for these unconventional superconductors has greatly intensified in the past few years as new candidate p-wave pairing states are proposed both intrinsically in bulk superconductors [5–15] and on the surfaces of more conventional superconductors [16–21].

The Little-Parks effect [22] originates from the macroscopic quantum coherence of Cooper pairs; due to the quantization of the fluxoid, the resistance of a thin superconducting ring oscillates as a function of the applied magnetic flux. For a conventional s-wave superconductor, the periodicity of these Little-Parks oscillations is given by the flux quantum $\Phi_0 = h/2e$, and the minima of the resistance correspond to integer multiples of Φ_0. It has been recognized, however, that unconventional superconductors may exhibit different kinds of Little-Parks oscillations. For example, in gapless superconductors with d-wave pairing, the Little-Parks oscillations acquire an enlarged periodicity $2\Phi_0$ [23–25], while polycrystalline p-wave superconductors have shifted Little-Parks oscillations with the minima of the resistance

corresponding to half-integer multiples of Φ_0 [13,14,26]. Fractional Little-Parks oscillations with reduced periodicities Φ_0/n have also been recently reported both experimentally [27] and theoretically [28–30].

For intrinsic spin-triplet p-wave superconductors, Majorana bound states have been predicted to emerge in the cores of half-quantum vortices (HQVs) at which half-integer flux quanta $\Phi_0/2$ pierce through the superconductor [2,3]. In the presence of such HQVs, the Little-Parks oscillations are then expected to possess a distinctive two-peak structure with minima of the resistance at both integer and half-integer multiples of Φ_0 [31–33]. At each half-integer minimum, the fluxoid of the superconducting ring is quantized to a half-integer multiple of Φ_0 (meaning that an HQV is bound to the central hole of the ring), while the two peaks around such a minimum correspond to transitions between integer and half-integer fluxoid quantizations. Nevertheless, while this two-peak structure in the Little-Parks oscillations may prove crucial for identifying spin-triplet superconductors, the precise conditions required for its observation are yet to be firmly established. More generally, a rigorous theoretical understanding of the spin-triplet Little-Parks effect could reveal additional signatures of spin-triplet superconductivity and hence provide alternative avenues for detecting this exotic state of matter on the device scale.

In this work, we use the Ginzburg-Landau approach to theoretically study the Little-Parks effect in spin-triplet superconducting rings supporting HQVs. We investigate both the "conventional" Little-Parks oscillations of the critical temperature itself [22] and the analogous magnetoresistance

*huac@ornl.gov
†halaszg@ornl.gov

oscillations below the critical temperature that result from thermal vortex tunneling [33–37]. When computing the residual resistance of the superconducting ring below the critical temperature, we not only focus on the lowest-energy fluxoid state [33,38], but account for all the thermally occupied fluxoid states and the thermally activated transitions between them.

We first demonstrate that HQVs are stabilized by appropriate higher-order terms in the Ginzburg-Landau free energy that, depending on their sign, may favor spin supercurrents over charge supercurrents. By examining how these terms affect the free energies of the various fluxoid states below the critical temperature, we confirm the presence of a two-peak structure in the magnetoresistance oscillations [31–33] and understand how the separation between the two peaks depends on the temperature. Next, we compute the magnetoresistance oscillations themselves and explicitly quantify the prominence of the characteristic two-peak structure. By identifying a fundamental trade-off between minimizing the width of each peak and maximizing the overall magnitude of the resistance, we provide detailed experimental guidelines for probing the two-peak structure in real candidate materials for spin-triplet superconductivity.

Turning to the "conventional" Little-Parks oscillations, we observe two separate critical temperatures, with the higher one marking the initial onset of superconductivity and the lower one separating spin-triplet superconducting states of a single spin species above and of both spin species below. Though the two-peak structure is absent from the Little-Parks oscillations of the upper critical temperature, it translates into a two-valley structure for the lower critical temperature, which is a further signature of spin-triplet superconductors supporting HQVs.

II. GINZBURG-LANDAU THEORY FOR A SPIN-TRIPLET SUPERCONDUCTOR

We consider a spin-triplet superconductor with $p_x + ip_y$ pairing symmetry in which spin-orbit coupling energetically favors $(\uparrow\uparrow)$ and $(\downarrow\downarrow)$ Cooper pairs over $(\uparrow\downarrow) + (\downarrow\uparrow)$ Cooper pairs [39]. Such a spin-triplet superconductor can support HQVs around which the superconducting phase of only one type of Cooper pair [either $(\uparrow\uparrow)$ or $(\downarrow\downarrow)$] winds by 2π. Under a magnetic field parallel to the spin quantization axis, the Ginzburg-Landau free energy of such a superconductor is given by [40]

$$
F = \frac{\phi T_c}{\Theta} \int d^3 r \Bigg\{ \sum_{\sigma=\uparrow,\downarrow} \Big[-\{(1-t) + z_\sigma |\boldsymbol{\nabla} \times \vec{a}|\} |\psi_\sigma|^2 + \frac{|\psi_\sigma|^4}{2} + \xi_0^2 \big|(\boldsymbol{\nabla} - i\vec{a})\psi_\sigma\big|^2 \Big]
$$
$$
+ c|\psi_\uparrow|^2 |\psi_\downarrow|^2 + \xi_0^2 [d_1 |(\boldsymbol{\nabla} - 2i\vec{a})[\psi_\uparrow \psi_\downarrow]|^2 + d_2 |\boldsymbol{\nabla}[\psi_\uparrow \psi_\downarrow^*]|^2] + \frac{\Theta}{2\mu_0 \phi T_c}(\boldsymbol{\nabla} \times \vec{a})^2 \Bigg\},
\tag{1}
$$

where $t = T/T_c$ is the dimensionless temperature (with T_c the critical temperature), ξ_0 is the zero-temperature coherence length, and $\vec{a} = 2\pi \vec{A}/\Phi_0$ is the magnetic vector potential, while $\psi_\uparrow$ and $\psi_\downarrow$ are the superconducting order parameters corresponding to the $(\uparrow\uparrow)$ and $(\downarrow\downarrow)$ Cooper pairs, respectively. The z_σ term arises from Zeeman splitting in a magnetic field with $z \equiv z_\uparrow = -z_\downarrow$, the c and $d_{1,2}$ terms describe coupling between the two types of Cooper pairs, and the last term of Eq. (1) accounts for the screening effect of the charge supercurrent. The dimensionless energy parameter ϕ is chosen such that ϕT_c is the condensation energy of the entire superconductor with volume Θ at zero temperature in the absence of a magnetic field ($\vec{a} = 0$) and any coupling ($c = d_1 = d_2 = 0$).

We point out that the standard form of the Ginzburg-Landau free energy [40] only contains terms in which the total number of order parameters ψ_σ and spatial derivatives $\boldsymbol{\nabla}$ does not exceed four. In this work, we include two additional symmetry-allowed terms proportional to $d_{1,2}$ with four order parameters and two spatial derivatives that energetically favor either charge supercurrents or spin supercurrents (depending on the sign of $d_{1,2}$). As we will later find, these additional terms are crucial for stabilizing HQVs. Other symmetry-allowed terms with the same number of order parameters and spatial derivatives do not affect the stability of HQVs and are thus omitted from Eq. (1). In the Appendix, we discuss the guiding principle to include high-order symmetry-allowed

terms in the Ginzburg-Landau free energy and determine the relevance of each of the symmetry-allowed terms to the stability of HQVs.

In the rest of this work, we focus on a thin superconducting ring of radius D and width $W \ll D$ in a perpendicularly applied magnetic field H (see Fig. 1). Assuming $W \ll \xi$, where $\xi = \xi_0(1-t)^{-1/2}$ is the finite-temperature coherence length, the order parameters ψ_σ only depend on the polar angle θ. Furthermore, if W is much smaller than the penetration
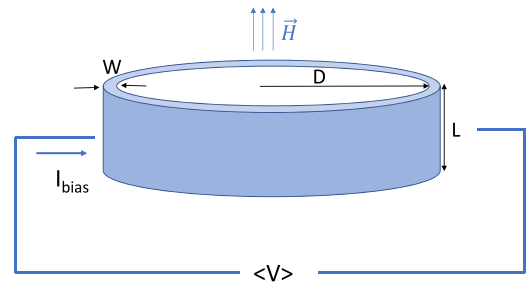
FIG. 1. Schematics of the Little-Parks experiment. The resistance of a thin superconducting ring with radius D, width $W \ll D$, and height L is measured as a function of the applied magnetic field $\vec{H}$ near the superconducting critical temperature. The resistance itself is determined by applying a bias current I_{bias} and measuring the resulting voltage $\langle V \rangle$.

TABLE I. Four families of solutions for the order parameters f_σ along with their respective free energies and physical interpretations. Each nontrivial family contains infinitely many distinct solutions labeled by the fluxoid numbers n_σ; the solutions for f_σ and the corresponding free energies depend on n_σ via $\tilde{\alpha}_\sigma(n_\sigma)$ and $\tilde{c}(n_\uparrow, n_\downarrow)$.

Solution	$f_\uparrow^2$	$f_\downarrow^2$	Free energy (F)	Physical interpretation
Trivial	0	0	0	Normal (nonsuperconducting) state
$(n_\uparrow)_\uparrow$	$\tilde{\alpha}_\uparrow$	0	$-\frac{1}{2}\phi T_c \tilde{\alpha}_\uparrow^2$	"Single-spin" triplet state with only ($\uparrow\uparrow$) Cooper pairs
$(n_\downarrow)_\downarrow$	0	$\tilde{\alpha}_\downarrow$	$-\frac{1}{2}\phi T_c \tilde{\alpha}_\downarrow^2$	"Single-spin" triplet state with only ($\downarrow\downarrow$) Cooper pairs
$(n_\uparrow, n_\downarrow)$	$\dfrac{\tilde{\alpha}_\uparrow - \tilde{c}\tilde{\alpha}_\downarrow}{1 - \tilde{c}^2}$	$\dfrac{\tilde{\alpha}_\downarrow - \tilde{c}\tilde{\alpha}_\uparrow}{1 - \tilde{c}^2}$	$-\frac{1}{2}\phi T_c \dfrac{\tilde{\alpha}_\uparrow^2 + \tilde{\alpha}_\downarrow^2 - 2\tilde{c}\tilde{\alpha}_\uparrow\tilde{\alpha}_\downarrow}{1 - \tilde{c}^2}$	"Two-spin" triplet state with both ($\uparrow\uparrow$) and ($\downarrow\downarrow$) Cooper pairs

depth λ, the screening effect of the charge supercurrent is negligible and the vector potential in the symmetric gauge is simply given by $\vec{A} = \frac{1}{2}DH\hat{\theta}$. Expressing the order parameters as $\psi_\sigma(\theta) = f_\sigma(\theta)e^{i\chi_\sigma(\theta)}$ in terms of the amplitudes $f_\sigma(\theta)$ and phases $\chi_\sigma(\theta)$, the Ginzburg-Landau equations derived from the free-energy functional of Eq. (1) are then

$$-\left[(1-t) + \frac{b_\sigma h}{\rho_0^2}\right]f_\sigma + f_\sigma^3 + cf_\sigma f_{-\sigma}^2 - \frac{1}{\rho_0^2}\left\{\frac{\partial^2 f_\sigma}{\partial\theta^2} - f_\sigma\left[\frac{\partial\chi_\sigma}{\partial\theta} - h\right]^2\right\} \tag{2a}$$

$$-\frac{d_1}{\rho_0^2}\left\{f_{-\sigma}\frac{\partial^2(f_\sigma f_{-\sigma})}{\partial\theta^2} - f_\sigma f_{-\sigma}^2\left[\frac{\partial(\chi_\sigma + \chi_{-\sigma})}{\partial\theta} - 2h\right]^2\right\} - \frac{d_2}{\rho_0^2}\left\{f_{-\sigma}\frac{\partial^2(f_\sigma f_{-\sigma})}{\partial\theta^2} - f_\sigma f_{-\sigma}^2\left[\frac{\partial(\chi_\sigma - \chi_{-\sigma})}{\partial\theta}\right]^2\right\} = 0,$$

$$\frac{\partial}{\partial\theta}\left\{f_\sigma^2\left[\frac{\partial\chi_\sigma}{\partial\theta} - h\right] + d_1(f_\sigma f_{-\sigma})^2\left[\frac{\partial(\chi_\sigma + \chi_{-\sigma})}{\partial\theta} - 2h\right] + d_2(f_\sigma f_{-\sigma})^2\left[\frac{\partial(\chi_\sigma - \chi_{-\sigma})}{\partial\theta}\right]\right\} = 0. \tag{2b}$$

Here, $b_\sigma = 2z_\sigma/\xi_0^2$ is a dimensionless Zeeman splitting, $\rho_0 = D/\xi_0$ is a dimensionless ring radius, and $h = HD^2\pi/\Phi_0$ is the number of flux quanta going through the ring, while $-\sigma$ indicates the opposite type of Cooper pair with respect to σ. We note that the conserved quantity within the curly brackets of Eq. (2b) is a supercurrent that corresponds to the given type of Cooper pair [($\uparrow\uparrow$) or ($\downarrow\downarrow$)]; the charge and spin supercurrents are then symmetric and antisymmetric combinations of these individual supercurrents, respectively. Since the order parameters $\psi_\sigma(\theta)$ must be single valued, the Ginzburg-Landau equations in Eq. (2) are also supplemented with the boundary conditions $f_\sigma(\pi) = f_\sigma(-\pi)$ and $\chi_\sigma(\pi) - \chi_\sigma(-\pi) = 2\pi n_\sigma$, where n_σ are arbitrary integers.

III. FIELD-INDUCED OSCILLATIONS OF THE CRITICAL TEMPERATURE

In this section, we consider the conventional Little-Parks oscillations [22] in the critical temperature of a spin-triplet superconducting ring as a function of the applied magnetic field. To describe these Little-Parks oscillations, we must establish the equilibrium phase diagram of the system by enumerating and comparing the stable solutions of Eq. (2) that correspond to local minima of the free-energy functional in Eq. (1). Such stable solutions take the general form of $f_\sigma(\theta) = $ const and $\chi_\sigma(\theta) = \chi_\sigma^{(0)} + n_\sigma\theta$, where $n_\sigma \in \mathbb{Z}$ are the fluxoid numbers for the two types of Cooper pairs and $\chi_\sigma^{(0)}$ are arbitrary reference phases [41]. Substituting this form into Eq. (2a), the constant values of the order parameters f_σ are then solutions

of the algebraic equations

$$f_\uparrow[f_\uparrow^2 + \tilde{c}(n_\uparrow, n_\downarrow)f_\downarrow^2 - \tilde{\alpha}_\uparrow(n_\uparrow)] = 0,$$
$$f_\downarrow[f_\downarrow^2 + \tilde{c}(n_\uparrow, n_\downarrow)f_\uparrow^2 - \tilde{\alpha}_\downarrow(n_\downarrow)] = 0, \tag{3}$$

where $\tilde{\alpha}_\sigma(n_\sigma) = (1-t) - \rho_0^{-2}[(n_\sigma - h)^2 - b_\sigma h]$ and $\tilde{c}(n_\uparrow, n_\downarrow) = c + \rho_0^{-2}[d_1(n_\uparrow + n_\downarrow - 2h)^2 + d_2(n_\uparrow - n_\downarrow)^2]$. These equations have four families of solutions that are listed in Table I along with their free energies and physical interpretations. The trivial solution with $f_\uparrow = f_\downarrow = 0$ corresponds to a normal state, while the three nontrivial families describe superconducting states. For the $(n_\uparrow)_\uparrow$ and $(n_\downarrow)_\downarrow$ solutions, only one spin species (either $\uparrow$ or $\downarrow$) forms Cooper pairs with the other spin species remaining in a normal state. These solutions correspond to a spin-triplet superconductor with only ($\uparrow\uparrow$) or ($\downarrow\downarrow$) pairing that can only support full quantum vortices (FQVs) with a single-integer fluxoid number ($n_\uparrow$ or $n_\downarrow$). In contrast, for the $(n_\uparrow, n_\downarrow)$ solutions, both spin species form Cooper pairs and the result is a spin-triplet superconductor with both ($\uparrow\uparrow$) and ($\downarrow\downarrow$) pairing. Introducing the charge $n_c = (n_\uparrow + n_\downarrow)/2$ and spin $n_s = (n_\uparrow - n_\downarrow)/2$ fluxoid numbers, and recognizing that n_c is the "usual" fluxoid number connected to the magnetic field, it is then clear that such a spin-triplet superconductor can support both FQVs (integer $n_{c,s}$) and HQVs (half-integer $n_{c,s}$).

To determine the equilibrium (i.e., lowest-free-energy) state of the ring, we need to compare the free energies of all solutions in Table I while keeping in mind that each solution is only physical if $f_\uparrow^2 \geqslant 0$ and $f_\downarrow^2 \geqslant 0$. The resulting equilibrium phase diagrams as a function of the temperature t, the
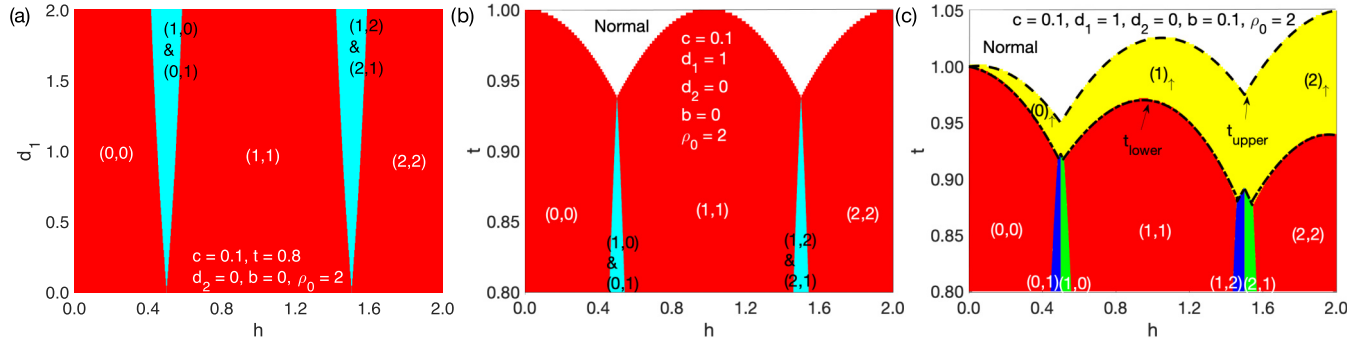
FIG. 2. Phase diagram of the lowest-free-energy fluxoid state (a) as a function of magnetic flux h and coupling coefficient d_1 without Zeeman splitting ($b = 0$), (b) as a function of magnetic flux h and temperature t without Zeeman splitting, and (c) as a function of h and t with Zeeman splitting ($b \neq 0$). Note that $d_2 < 0$ has the same effect as $d_1 > 0$. The white area marks the normal state, the yellow area marks a single-spin triplet state with $f_\downarrow^2 = 0$, and the red area marks a two-spin triplet state with an integer fluxoid (FQV) around the ring ($n_{c,s} \in \mathbb{Z}$). In (a) and (b), the light-blue area indicates a degeneracy between two half-integer fluxoid (HQV) states with $n_s = \pm 1/2$, while in (c), the green (blue) color means that the HQV state with $n_s = +1/2$ ($n_s = -1/2$) is the lowest-free-energy state. In (c), the dashed and dash-dotted lines mark the upper and lower critical temperatures [Eqs. (7) and (8)], respectively. Note that the dimensionless radius ρ_0 is kept relatively small here so that the oscillations in the critical temperatures can be clearly seen.

magnetic field h, and the coupling constants $d_{1,2}$ are plotted in Fig. 2. We start understanding these results by comparing the various solutions within each family of Table I. For the "single-spin" states $(n_\uparrow)_\uparrow$ and $(n_\downarrow)_\downarrow$ (yellow shaded area in Fig. 2), the free energy takes the exact form

$$F_{(n_\sigma)_\sigma} = -\frac{\phi T_c}{2} \left\{ (1 - t) - \frac{1}{\rho_0^2} [(n_\sigma - h)^2 - b_\sigma h] \right\}^2. \quad (4)$$

$$F_{(n_\uparrow, n_\downarrow)} = \phi T_c \left\{ -\frac{(1-t)^2}{1+c} + \frac{2(1-t)}{\rho_0^2} \frac{[(1+c) + 2(1-t)d_2]n_s^2 + [(1+c) + 2(1-t)d_1](n_c - h)^2}{(1+c)^2} + O(\rho_0^{-4}) \right\}. \quad (5)$$

Therefore, in the $\rho_0 \gg 1$ limit, we can restrict our attention to the FQV states with $n_s = 0$ and the HQV states with $n_s = \pm 1/2$ as all other states are penalized by the term $\propto n_s^2$. If we then assume $n \leqslant h \leqslant n + 1$ (with $n \in \mathbb{Z}$ and $n \geqslant 0$) again, the lowest-energy FQV state has $n_c = n$ for $h < n + 1/2$, and $n_c = n + 1$ for $h > n + 1/2$. These two states correspond to (n, n) and $(n + 1, n + 1)$ in the notation of Table I and are both denoted by red in Fig. 2. The two lowest-energy HQV states with $n_c = n + 1/2$ and $n_s = \pm 1/2$, corresponding to $(n + 1, n)$ and $(n, n + 1)$, are degenerate up to $O(\rho_0^{-2})$. This degeneracy is split by a higher-order term in the free energy, $4\rho_0^{-4} bhn_s(n_c - h)/(1 - c)$, such that the lowest-energy HQV state is $(n, n + 1)$ for $h < n + 1/2$ (blue in Fig. 2) and $(n + 1, n)$ for $h > n + 1/2$ (green in Fig. 2). To compare the lowest-energy FQV and HQV states with one another, we finally recognize that the terms $\propto n_s^2$ and $\propto (n_c - h)^2$ have relative coefficients $(1 + c) + 2(1 - t)d_2$ and $(1 + c) + 2(1 - t)d_1$ in Eq. (5). Given that $n_s^2 = 1/4$ ($n_s^2 = 0$) for the HQV (FQV) state and $0 \leqslant (n_c - h)^2 \leqslant 1/4$ for both states, the HQV state can only have lower energy than the FQV state if $d_1 - d_2 > 0$. Therefore, as previously stated, the coupling constants $d_{1,2}$ are crucial for stabilizing HQV states. Specifically, a HQV state can only be

We emphasize that the expression inside the curly brackets must be positive for the given state to be valid. Hence, assuming $n \leqslant h \leqslant n + 1$ (where n is a non-negative integer) without loss of generality, the single-spin state with the lowest free energy at any finite Zeeman splitting $b > 0$ (where $b \equiv b_\uparrow = -b_\downarrow$) is $(n)_\uparrow$ if $h < n + 1/2$, and $(n + 1)_\uparrow$ if $h > n + 1/2$. For the "two-spin" states $(n_\uparrow, n_\downarrow)$, we can expand the free energy up to $O(\rho_0^{-2})$ and express n_σ in terms of $n_{c,s}$ to obtain

energetically favorable if $d_1 > 0$ and/or $d_2 < 0$. For $d_1 - d_2 > 0$, the lowest-energy two-spin state is then a HQV state within the field range $n + 1/2 - \Delta h/2 < h < n + 1/2 + \Delta h/2$ characterized by the width parameter

$$\Delta h = \frac{(1 - t)(d_1 - d_2)}{(1 + c) + 2(1 - t)d_1} + O(\rho_0^{-2}). \quad (6)$$

As shown by Eq. (6) and Fig. 2, the field range within which a HQV state is energetically favorable increases as the temperature t is lowered and as the magnitudes of the coupling constants $d_{1,2}$ are increased. Conversely, the field range vanishes both at the critical temperature ($t \to 1$) and when the coupling constants vanish ($d_{1,2} \to 0$). We further remark that the coupling constants $d_{1,2}$ are generically expected to be $O(1)$ and that $|d_{1,2}| \sim 1$ are consistent with the width of half-height magnetization steps reported in Ref. [8] for the candidate material Sr_2RuO_4.

We are now ready to understand the field dependence of the critical temperature. We start by recognizing that for $bh \neq 0$, there are in fact two critical temperatures; in addition to the upper critical temperature at which superconductivity first appears for one spin species, there is a lower critical temperature at which the other spin species also becomes superconducting. These two critical temperatures can be readily determined by
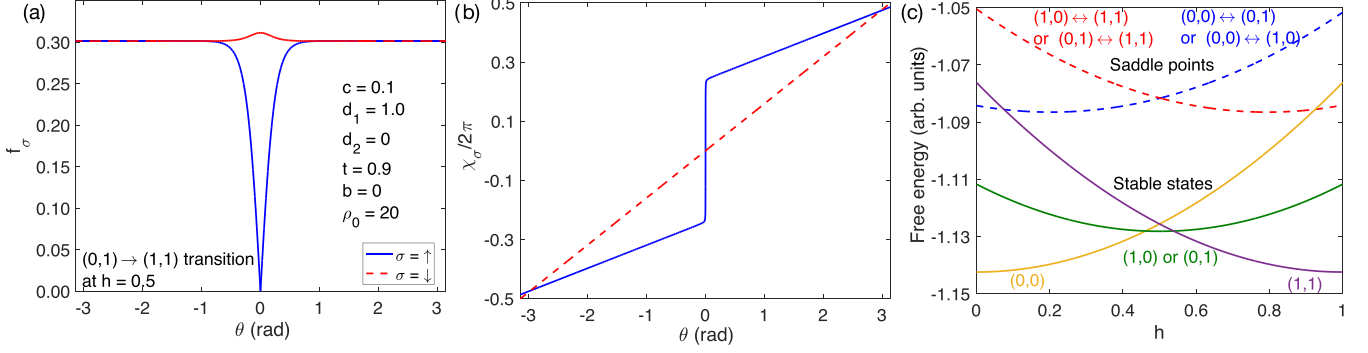
FIG. 3. (a), (b) Saddle-point solutions for (a) the amplitude and (b) the phase of the superconducting order parameters $\psi_\uparrow$ and $\psi_\downarrow$ as the fluxoid numbers $(n_\uparrow, n_\downarrow)$ change from (0,1) to (1,1) at magnetic flux $h = 0.5$. (c) Free energies of the relevant stable states (solid lines) and the saddle points connecting them (dashed lines) as a function of the magnetic flux h.

comparing the free energies of the lowest-energy single-spin and two-spin superconducting states [see Eqs. (4) and (5)] with each other and with the free energy of the normal state (which is zero). The upper critical temperature reads

$$t_{\text{upper}} = 1 + \frac{1}{\rho_0^2}[b|h| - (h - \lfloor h \rceil)^2], \qquad (7)$$

where $\lfloor h \rceil$ is h rounded to the nearest integer. This critical temperature has the same field-induced oscillation as the critical temperature of a spin-singlet superconductor [22] except for an additional linear increase with the field $|h|$ that shifts the maxima around integer h [see Fig. 2(c)]. Up to $O(\rho_0^{-4})$, the lower critical temperature takes the form

$$t_{\text{lower}} = 1 - \frac{[h - f(h)]^2 - c(h - \lfloor h \rceil)^2 + (1 + c)b|h|}{\rho_0^2(1 - c)}$$
$$- \frac{\{d_1[2h - \lfloor h \rceil - f(h)]^2 + d_2[\lfloor h \rceil - f(h)]^2\}\{[h - f(h)]^2 - (h - \lfloor h \rceil)^2 + 2b|h|\}}{\rho_0^4(1 - c)^2} + O(\rho_0^{-6}) \qquad (8)$$

in terms of the piecewise continuous function

$$f(h) = \begin{cases} \lfloor h \rceil & \text{if } |h - \lfloor h \rceil| < (1 - \Delta h)/2, \\ \lfloor 2h \rceil - \lfloor h \rceil & \text{if } |h - \lfloor h \rceil| > (1 - \Delta h)/2, \end{cases} \qquad (9)$$

where the upper and lower cases correspond to transitions into the FQV and HQV states, respectively, and the field ranges around half-integer h with transitions into HQV states are controlled by the width parameter,

$$\Delta h = \frac{2(d_1 - d_2)b|h|}{\rho_0^2(1 - c)} + O(\rho_0^{-4}). \qquad (10)$$

In contrast to the upper critical temperature, the lower critical temperature shows an overall decrease with the field $|h|$ and contains additional maxima at all half-integer values of h [see Fig. 2(c)] around which the transitions into the HQV states happen. We emphasize that while Eqs. (6) and (10) describe the same width parameter Δh, one cannot obtain Eq. (10) by simply substituting Eq. (8) into Eq. (6) because the leading term of Eq. (10) is $O(\rho_0^{-2})$, whereas Eq. (6) is only accurate up to $O(1)$ terms. We also remark that a spin-singlet superconductor with multiple bands does not have two separate critical temperatures because its Ginzburg-Landau free energy includes bilinear coupling terms between different order parameters [42]. In contrast, such coupling terms of the form $\propto \psi_{-\sigma}^* \psi_\sigma$ are forbidden in our case by spin-rotation symmetry around the field direction (i.e., the direction perpendicular to the ring).

IV. MAGNETORESISTANCE OSCILLATIONS BELOW THE CRITICAL TEMPERATURE

In this section, we study the resistance of the superconducting ring in the spin-triplet state below the lower critical temperature in order to derive its oscillations as a function of the applied magnetic field. To do so, we will first consider thermal fluctuations in the order parameters $\psi_\sigma(\theta)$ that drive transitions between different free-energy minima. We will then use the computed transition rates to estimate the electrical resistance due to the resulting thermal decay of the charge supercurrent [41,43].

During a thermal transition from one free-energy minimum to another one, the system goes through an appropriate free-energy saddle point, and the free-energy barrier controlling the transition rate is simply the free-energy difference between the saddle point and the original minimum. The two free-energy minima connected by the thermal transition correspond to two stable solutions of Eq. (2) that differ in a fluxoid number n_σ. Therefore, the saddle-point solution must exhibit a phase slip in the corresponding order parameter $\psi_\sigma(\theta)$, i.e., a suppression of the amplitude $f_\sigma(\theta)$ around some angle θ. For a spin-singlet superconductor, an analytical expression for this saddle-point solution was found in Ref. [41]. Since the analytical solution only applies for a spin-triplet superconductor in the absence of coupling terms ($c = d_{1,2} = 0$), we choose to solve Eq. (2) numerically with a combination
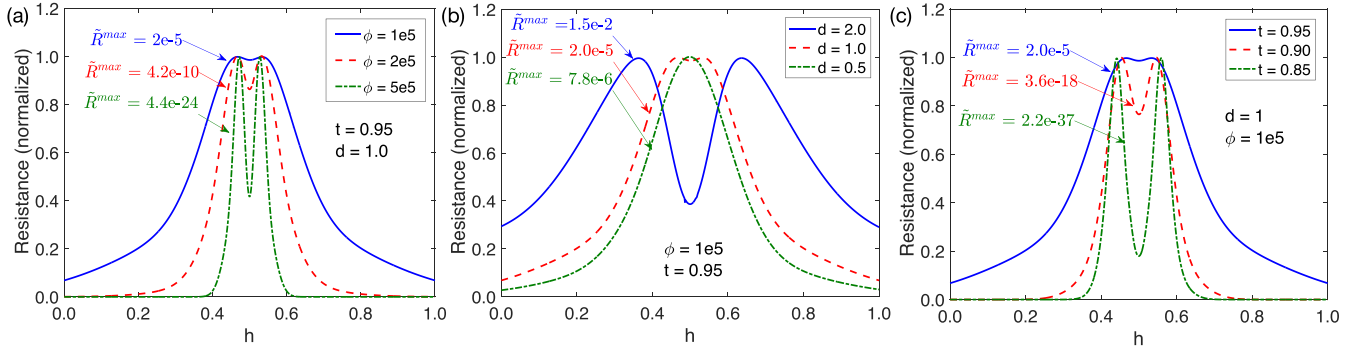
FIG. 4. Magnetoresistance oscillations of a spin-triplet superconducting ring for different values of (a) the dimensionless energy parameter (i.e., condensation energy) ϕ, (b) the coupling coefficient $d \equiv d_1 - d_2$, and (c) the dimensionless temperature t. The following parameter values apply to all three subfigures: $\rho_0 = 20$, $c = 0.1$, and $b = 0$. The dimensionless resistance, $\tilde{R} = R/R_0$, is calculated from Eq. (14) and normalized by its maximum value, $\tilde{R}^{\max}$, which is specified for each resistance curve. Note that since the resistance prefactor is $R_0 \sim 10^5 \, \Omega$, the resistance curves with $\tilde{R}^{\max} \ll 10^{-5}$ are not expected to be experimentally observable and are only included to show the general trends in the behavior of the two-peak structure.

of a shooting method and an adaptive step-size Runge-Kutta integration scheme.

An example of the numerically obtained saddle-point solution is depicted in Figs. 3(a) and 3(b). This solution corresponds to a transition between two stable solutions with respective fluxoid numbers $(n_\uparrow, n_\downarrow) = (0, 1)$ and $(1,1)$. Since $n_\uparrow$ changes from 0 to 1 while $n_\downarrow$ remains the same, $f_\uparrow$ goes through a strong suppression in a region of size $\xi = \xi_0(1 - t)^{-1/2}$ around $\theta = 0$, whereas $f_\downarrow$ is only slightly perturbed around its stable constant solution.

Once the saddle-point configurations of $\psi_\uparrow$ and $\psi_\downarrow$ are found for a transition between $(n_\uparrow, n_\downarrow)$ and $(n'_\uparrow, n'_\downarrow)$, the saddle-point free energy associated with this transition, $F_{(n_\uparrow, n_\downarrow) \leftrightarrow (n'_\uparrow, n'_\downarrow)}$, can be calculated through Eq. (1). For the stable solutions with fluxoid numbers $0 \leqslant n_\sigma \leqslant 1$ and the saddle-point solutions connecting them, the free energies are plotted in Fig. 3(c) as a function of the field h. We remark that there is an exact degeneracy between $(n_\uparrow, n_\downarrow) = (0, 1)$ and $(1,0)$ because we neglect the Zeeman splitting by setting $b = 0$ in this section.

Given that the free-energy barrier is simply given by $\Delta F_{(n_\uparrow, n_\downarrow) \to (n'_\uparrow, n'_\downarrow)} = F_{(n_\uparrow, n_\downarrow) \leftrightarrow (n'_\uparrow, n'_\downarrow)} - F_{(n_\uparrow, n_\downarrow)}$ for the transition

from $(n_\uparrow, n_\downarrow)$ to $(n'_\uparrow, n'_\downarrow)$, the thermally activated rate of this transition can be written as [28,43]

$$\Gamma_{(n_\uparrow, n_\downarrow) \to (n'_\uparrow, n'_\downarrow)} = \Omega P_{(n_\uparrow, n_\downarrow)} \exp[-\beta \Delta F_{(n_\uparrow, n_\downarrow) \to (n'_\uparrow, n'_\downarrow)}], \quad (11)$$

where $\Omega \sim (T_c/\hbar)(1 - t)^{9/4}(\phi \rho_0)^{1/2}$ [41,43] is an overall temperature-dependent prefactor, $\beta = 1/T$ is the inverse temperature, and $P_{(n_\uparrow, n_\downarrow)}$ is the probability of the superconducting ring to be in the stable state $(n_\uparrow, n_\downarrow)$. At any finite temperature, this probability is given by

$$P_{(n_\uparrow, n_\downarrow)} = \frac{1}{Z} \exp[-\beta F_{(n_\uparrow, n_\downarrow)}],$$
$$Z = \sum_{n_\uparrow, n_\downarrow} \exp[-\beta F_{(n_\uparrow, n_\downarrow)}]. \quad (12)$$

In the presence of a small bias current I_{bias} applied to a section of the ring, the free-energy barrier takes the modified form [43] $\Delta \tilde{F}_{(n_\uparrow, n_\downarrow) \to (n'_\uparrow, n'_\downarrow)} = \Delta F_{(n_\uparrow, n_\downarrow) \to (n'_\uparrow, n'_\downarrow)} - (\delta n_\uparrow + \delta n_\downarrow)\Phi_0 I_{\text{bias}}/4$, where $\delta n_\sigma \equiv n'_\sigma - n_\sigma$. The mean voltage $\langle V \rangle$ between the two end points of the section due to repeated phase slips is then [28,43]

$$\langle V \rangle = \frac{\Omega \Phi_0}{2} \sum_{n_\uparrow, n_\downarrow} P_{(n_\uparrow, n_\downarrow)} \sum_{n'_\uparrow, n'_\downarrow} (\delta n_\uparrow + \delta n_\downarrow) \exp\left[-\beta \Delta F_{(n_\uparrow, n_\downarrow) \to (n'_\uparrow, n'_\downarrow)} + \beta(\delta n_\uparrow + \delta n_\downarrow)\frac{\Phi_0 I_{\text{bias}}}{4}\right]. \quad (13)$$

Finally, assuming $I_{\text{bias}} \ll T/\Phi_0$, we can expand $\langle V \rangle$ up to first order in I_{bias} and obtain the effective resistance as

$$R = \frac{\langle V \rangle}{I_{\text{bias}}} = R_0 \frac{\sum_{n_\uparrow, n_\downarrow} \left\{ \sum_{\delta n_\uparrow = \pm 1} \delta n_\uparrow^2 \exp[-\beta F_{(n_\uparrow, n_\downarrow) \leftrightarrow (n_\uparrow + \delta n_\uparrow, n_\downarrow)}] + \sum_{\delta n_\downarrow = \pm 1} \delta n_\downarrow^2 \exp[-\beta F_{(n_\uparrow, n_\downarrow) \leftrightarrow (n_\uparrow, n_\downarrow + \delta n_\downarrow)}] \right\}}{\sum_{n_\uparrow, n_\downarrow} \exp[-\beta F_{(n_\uparrow, n_\downarrow)}]}, \quad (14)$$

where $R_0 = \beta \Omega \Phi_0^2/8$. In this final step, we ignore transitions that involve both fluxoid numbers n_σ or change either fluxoid number by more than 1 as these transitions have larger free-

energy barriers and their contributions to the resistance are thus negligible.

Figure 4 shows the magnetoresistance calculated from Eq. (14) at different values of the temperature t, the coupling

constants $d_{1,2}$, and the energy parameter ϕ. Since the relevant coupling constant for stabilizing HQVs has been found to be $d \equiv d_1 - d_2$, we set $d_2 = 0$ for simplicity and only consider $d_1 = d$ in this section.

In Fig. 4, we readily observe the expected two-peak structure in the magnetoresistance oscillations [31–33] and recognize clear trends in its behavior as a function of t, d, and ϕ. We first consider the separation between the two peaks that depends on t and d, but not on ϕ. As understood in previous works [31–33], each peak corresponds to a transition between a FQV state and a HQV state, with a HQV state being energetically favored in the narrow range between the two peaks. Hence, we immediately identify the separation between the two peaks as the width parameter Δh in Eq. (6) and understand that for $d(1 - t) \ll 1$, it is linearly proportional to both the coupling constant d and the temperature difference $1 - t$ with respect to the critical temperature.

We next focus on the width of each peak, δh, which, in conjunction with the peak separation Δh, determines how well the two peaks are distinguishable. We generally observe in Fig. 4 that the peaks broaden if ϕ is decreased or t is increased. To understand this result, we first notice from Eq. (14) that each peak extends over a field range in which the free-energy difference between the two lowest-energy fluxoid states $(n_\uparrow, n_\downarrow)$ is smaller than the temperature T; the resistance has a peak within such a field range because thermal phase slips between the two highly occupied lowest-energy states occur with an enhanced rate. Then, using Eq. (5) and assuming $\rho_0 \gg 1$ as well as $|1 - t| \ll 1$, we find $|\partial F_{(n_\uparrow, n_\downarrow)}/\partial h| \sim \phi T_c (1 - t) \rho_0^{-2}$ and estimate the peak width as $\delta h \sim T/|\partial F_{(n_\uparrow, n_\downarrow)}/\partial h| \sim \rho_0^2/[\phi(1 - t)]$. The conclusion is that as shown by Fig. 4, the peak width is inversely proportional to both the energy parameter ϕ and the temperature difference $1 - t$ with respect to the critical temperature.

The two peaks are well distinguishable if the peak separation Δh is at least as large as the peak width δh. From the above analysis, this condition corresponds to a lower bound for the coupling constant: $d \gtrsim \rho_0^2/[\phi(1 - t)^2]$. We note though that the energy parameter ϕ is proportional to the total volume Θ of the superconducting ring and can, in principle, be made arbitrarily large by increasing the out-of-plane ring height L. We also remark that for a reasonable ring radius $D \sim 1$ μm, the peak separation $\Delta h \sim 0.1$ seen in Fig. 4 corresponds to an approximately 0.1 mT change in the applied magnetic field.

However, even if the two peaks are well distinguishable, the two-peak structure in the resistance may still not be observable if the overall magnitude of the resistance is prohibitively small. In particular, Fig. 4 shows that the magnitude of the resistance is strongly suppressed for large ϕ and/or small t. From Eq. (14), the magnitude of the resistance is determined by the free-energy difference between the relevant stable and saddle-point solutions (i.e., the free-energy barrier). Since the saddle-point solutions have a localized suppression of superconductivity in a region of size $\xi = \xi_0 (1 - t)^{-1/2}$ with respect to the stable solutions, this free-energy difference can be estimated as $\delta F \sim |F_{(n_\uparrow, n_\downarrow)}|\xi/D \sim \phi T_c (1 - t)^{3/2} \rho_0^{-1}$ if we assume $\rho_0 \gg 1$ and $|1 - t| \ll 1$ once again. The magnitude of the resistance is then exponentially small [see Eq. (14)] when

$\beta \delta F \sim \phi (1 - t)^{3/2} \rho_0^{-1} \sim \rho_0 (1 - t)^{1/2}/\delta h \gg 1$. Interestingly, this result reveals a fundamental trade-off between increasing the magnitude of the resistance and decreasing the peak width, which are both important for observing the two-peak structure in the resistance.

Nevertheless, Fig. 4 shows that a discernible two-peak structure with a reasonable magnitude of the resistance is possible for appropriate values of the parameters. Indeed, for $\rho_0 \sim 10$, $t \sim 0.9$, and $\phi \sim 10^5$, the resistance prefactor in Eq. (14) is $R_0 \sim (\hbar/e^2)(1 - t)^{9/4}(\phi \rho_0)^{1/2} \sim 10^5$ Ω, and the largest resistance magnitudes seen in Fig. 4 are therefore larger than 1 Ω. For a small enough bias current $I_{\text{bias}} \sim 1$ nA, required by $I_{\text{bias}} \ll T_c/\Phi_0$ with $T_c \sim 1$ K, the measured voltage $\langle V \rangle$ is then at least 1 nV, i.e., within the sensitivity of a typical transport measurement.

V. DISCUSSION AND OUTLOOK

In this work, we employed the Ginzburg-Landau approach to study the Little-Parks magnetoresistance oscillations of spin-triplet superconductors in the presence of HQVs harboring Majorana bound states. Focusing on a ring geometry with a sufficiently small width ($W \ll \xi, \lambda$), we first constructed the appropriate Ginzburg-Landau free energy and identified two specific higher-order terms [the ones proportional to $d_{1,2}$ in Eq. (1)] that are critical for stabilizing HQVs. Then, we used the corresponding Ginzburg-Landau equations to derive both the conventional Little-Parks oscillations of the superconducting critical temperature [22] and the closely related oscillations in the residual resistance due to thermal vortex tunneling below the critical temperature [33–37].

Our main result is a rigorous theoretical underpinning of the distinctive two-peak structure that the magnetoresistance oscillations are expected to possess [31–33]. The two peaks demarcate a narrow field range of width Δh [see Eq. (6)] within which it is energetically favorable to bind a HQV to the central hole of the superconducting ring. Because HQVs are stabilized by higher-order terms in the Ginzburg-Landau free energy, the peak separation Δh is linearly proportional not only to the appropriate coupling constant $d_1 - d_2$, but also to the relative temperature $1 - t$ with respect to the critical temperature. In other words, the two-peak structure is observable in the magnetoresistance oscillations below the critical temperature, but not in the conventional Little-Parks oscillations of the critical temperature itself.

We next established the most general conditions under which the two-peak structure in the magnetoresistance oscillations is expected to be experimentally discernible in a real superconductor. Specifically, we identified a fundamental trade-off between making the peaks sufficiently narrow (hence, well distinguishable) and ensuring that the overall magnitude of the resistance is not overly suppressed. For the parameter values $\rho_0 = D/\xi_0 \sim 10$ and $t = T/T_c \sim 0.9$ used in Fig. 4, we find that this trade-off corresponds to energy parameter $\phi \sim 10^5$. Since ϕT_c is defined as a total condensation energy at zero temperature, this quantity is of the order of $\nu \Delta^2 \sim \nu T_c^2$, where ν is the electronic density of states at the Fermi level and Δ is the superconducting pairing gap. Therefore, we readily obtain $\phi \sim \nu T_c \sim \Theta T_c/(a^3 E_F)$, where

Θ is the ring volume, a is the lattice constant, and E_F is the Fermi energy. For $T_c \sim 1$ K, $a \sim 1$ nm, and $E_F \sim 0.1$ eV, the ideal energy parameter $\phi \sim 10^5$ then corresponds to ring volume $\Theta \sim 0.1$ μm^3, which is achieved, for example, by setting the radius, width, and height of the ring to $D \sim 1$ μm, $W \sim 100$ nm, and $L \sim 100$ nm, respectively. Using these values for the parameters, the overall magnitude of the resistance is $R \gtrsim 1$ Ω and the required resolution in the applied magnetic field is $\Delta H \sim 0.1$ mT.

Though the critical temperature marking the onset of superconductivity (i.e., the upper critical temperature) does not have a distinctive structure in its Little-Parks oscillations, we also found a lower critical temperature that separates superconducting states of a single-spin species above and of both spin species below. In turn, this lower critical temperature has two distinct minima around each half-integer value of h [see Fig. 2(c)], which correspond to the two peaks in the related magnetoresistance oscillations [44]. To experimentally determine the lower critical temperature, one would need to selectively measure the electrical resistance of the spin species that is normal above and superconducting below the transition. For example, one could apply the bias current through half-metallic leads that can only emit or absorb one spin species but not the other one. We also emphasize that this measurement would require a sharp superconducting transition with no residual resistance due to vortex tunneling below. As such, it would be in a different regime and need a much larger ring volume Θ than discussed above. Since the radius and the width are restricted to $D \lesssim 1$ μm and $W \lesssim 100$ nm by other considerations, this measurement would then correspond to a cylindrical geometry with a large height $L \gg 1$ μm as in the original Little-Parks experiment [22].

Physically, the higher-order terms proportional to $d_{1,2}$ in the Ginzburg-Landau free energy stabilize HQVs by favoring spin supercurrents over charge supercurrents (for the right signs of $d_{1,2}$). In this sense, they play an analogous role to the ratio of the spin and charge superfluid densities, $\gamma = \rho_{sp}/\rho_s$, in the London limit [28,45]. Indeed, from a comparison of Eq. (5) in this work and Eq. (15) in Ref. [28], we can identify the superfluid-density ratio as $\gamma = [(1+c) + 2(1-t)d_2]/[(1+c) + 2(1-t)d_1]$, which is consistent with the general expectation that $\gamma \to 1$ at the critical temperature [31]. Since it is also expected on general grounds that $\gamma < 1$ for interacting superconductors [45–47], we anticipate that

as a result of $d_1 > d_2$, our results apply to any spin-triplet superconductor in which (↑↑) and (↓↓) Cooper pairs are energetically favored over (↑↓) + (↓↑) Cooper pairs. In the future, it would be interesting to understand how our results connect to the London limit and, in particular, how the fractional magnetoresistance oscillations in the presence of disorder predicted in Ref. [28] can be recovered from our general Ginzburg-Landau approach. This connection could then be used to establish the general conditions under which the fractional magnetoresistance oscillations are experimentally observable.

APPENDIX: DETAILED ANALYSIS OF SYMMETRY-ALLOWED TERMS

Here we consider all symmetry-allowed terms with four order parameters and two spatial derivatives in the Ginzburg-Landau free energy and demonstrate that only the terms proportional to $d_{1,2}$ in Eq. (1) matter for the stability of HQVs. The symmetry-allowed terms with four order parameters and two spatial derivatives can be enumerated by (i) considering each symmetry-allowed term with four order parameters ($|\psi_\sigma|^4$ and $|\psi_\uparrow|^2|\psi_\downarrow|^2$), (ii) considering all possible ways of dividing the four order parameters into two pairs, and (iii) taking the gauge-covariant derivative of each pair such that each order parameter with (without) a complex conjugate contributes an additional term $+i\vec{a}$ ($-i\vec{a}$) to the derivative. Following this guiding principle, the general symmetry-allowed form of Ginzburg-Landau free energy [see Eq. (1)] can be written as

$$F = \frac{\phi T_c}{\Theta} \int d^3 r \left\{ \sum_{\sigma=\uparrow,\downarrow} \left[-\{(1-t) + z_\sigma |\nabla \times \vec{a}|\}|\psi_\sigma|^2 + \frac{|\psi_\sigma|^4}{2} + \xi_0^2 |(\nabla - i\vec{a})\psi_\sigma|^2 \right] + c|\psi_\uparrow|^2|\psi_\downarrow|^2 + \xi_0^2 [d_1|(\nabla - 2i\vec{a})[\psi_\uparrow\psi_\downarrow]|^2 \right.$$

$$\left. + d_2 |\nabla[\psi_\uparrow \psi_\downarrow^*]|^2 + d_3 \nabla|\psi_\uparrow|^2 \nabla|\psi_\downarrow|^2] + \frac{\xi_0^2}{2} \sum_{\sigma=\uparrow,\downarrow} [e_1|(\nabla - 2i\vec{a})\psi_\sigma^2|^2 + e_2(\nabla|\psi_\sigma|^2)^2] + \frac{\Theta}{2\mu_0 \phi T_c}(\nabla \times \vec{a})^2 \right\}, \quad \text{(A1)}$$

and the corresponding Ginzburg-Landau equations in terms of $\psi_\sigma(\theta) = f_\sigma(\theta)e^{i\chi_\sigma(\theta)}$ [see Eq. (2)] are given by

$$-\left[(1-t) + \frac{b_\sigma h}{\rho_0^2} \right] f_\sigma + f_\sigma^3 + cf_\sigma f_{-\sigma}^2 - \frac{1}{\rho_0^2} \left\{ \frac{\partial^2 f_\sigma}{\partial \theta^2} - f_\sigma \left[\frac{\partial \chi_\sigma}{\partial \theta} - h \right]^2 \right\}$$

$$-\frac{d_1}{\rho_0^2} \left\{ f_{-\sigma} \frac{\partial^2 (f_\sigma f_{-\sigma})}{\partial \theta^2} - f_\sigma f_{-\sigma}^2 \left[\frac{\partial(\chi_\sigma + \chi_{-\sigma})}{\partial \theta} - 2h \right]^2 \right\} - \frac{d_2}{\rho_0^2} \left\{ f_{-\sigma} \frac{\partial^2 (f_\sigma f_{-\sigma})}{\partial \theta^2} - f_\sigma f_{-\sigma}^2 \left[\frac{\partial(\chi_\sigma - \chi_{-\sigma})}{\partial \theta} \right]^2 \right\}$$

$$-\frac{d_3 f_\sigma}{\rho_0^2}\frac{\partial^2 (f_{-\sigma}^2)}{\partial \theta^2} - \frac{e_1}{\rho_0^2}\left\{ f_\sigma \frac{\partial^2 (f_\sigma^2)}{\partial \theta^2} - 4f_\sigma^3\left[\frac{\partial \chi_\sigma}{\partial \theta} - h\right]^2 \right\} - \frac{e_2 f_\sigma}{\rho_0^2}\frac{\partial^2 (f_\sigma^2)}{\partial \theta^2} = 0,$$

$$\frac{\partial}{\partial \theta}\left\{ f_\sigma^2\left[\frac{\partial \chi_\sigma}{\partial \theta} - h\right] + d_1 (f_\sigma f_{-\sigma})^2\left[\frac{\partial(\chi_\sigma + \chi_{-\sigma})}{\partial \theta} - 2h\right] + d_2 (f_\sigma f_{-\sigma})^2\left[\frac{\partial(\chi_\sigma - \chi_{-\sigma})}{\partial \theta}\right] + 2e_1 f_\sigma^4\left[\frac{\partial \chi_\sigma}{\partial \theta} - h\right] \right\} = 0. \quad (A2)$$

Focusing on the stable solutions with $f_\sigma(\theta) = \text{const}$ and $\chi_\sigma(\theta) = \chi_\sigma^{(0)} + n_\sigma \theta$ (where $n_\sigma \in \mathbb{Z}$), the free energy up to $O(\rho_0^{-2})$ in terms of $n_c = (n_\uparrow + n_\downarrow)/2$ and $n_s = (n_\uparrow - n_\downarrow)/2$ [see Eq. (5)] is then found to be

$$F_{(n_\uparrow, n_\downarrow)} = \phi T_c\left\{ -\frac{(1-t)^2}{1+c} + \frac{2(1-t)}{\rho_0^2}\frac{[(1+c)+2(1-t)(d_2+e_1)]n_s^2 + [(1+c)+2(1-t)(d_1+e_1)](n_c-h)^2}{(1+c)^2} + O(\rho_0^{-4}) \right\}.$$

$$(A3)$$

We first notice that the coefficients d_3 and e_2 are absent from Eq. (A3). Since the corresponding terms in the Ginzburg-Landau free energy only contain derivatives of the form $\nabla|\psi_\sigma|^2$, they do not contribute to the free energy for the stable solutions characterized by $|\psi_\sigma| = \text{const}$. We next recognize that the terms $\propto (n_c - h)^2$ and $\propto n_s^2$ in Eq. (A3) penalize charge supercurrents and spin supercurrents, respectively. Since the coefficient e_1 has the same contribution to both terms, it does not favor either charge supercurrents or spin supercurrents and therefore does not affect the stability of HQVs. In contrast, the coefficients d_1 and d_2 only penalize charge supercurrents and spin supercurrents, respectively. Hence, as found in the main text, HQVs can be stabilized for $d_1 > 0$ and/or $d_2 < 0$.

[1] C. Nayak, S. H. Simon, A. Stern, M. Freedman, and S. Das Sarma, Non-Abelian anyons and topological quantum computation, Rev. Mod. Phys. **80**, 1083 (2008).

[2] N. Read and D. Green, Paired states of fermions in two dimensions with breaking of parity and time-reversal symmetries and the fractional quantum Hall effect, Phys. Rev. B **61**, 10267 (2000).

[3] D. A. Ivanov, Non-Abelian Statistics of Half-Quantum Vortices in p-Wave Superconductors, Phys. Rev. Lett. **86**, 268 (2001).

[4] J. Alicea, New directions in the pursuit of Majorana fermions in solid state systems, Rep. Prog. Phys. **75**, 076501 (2012).

[5] Y. Maeno, H. Hashimoto, K. Yoshida, S. Nishizaki, T. Fujita, J. G. Bednorz, and F. Lichtenberg, Superconductivity in a layered perovskite without copper, Nature (London) **372**, 532 (1994).

[6] Y. Maeno, T. M. Rice, and M. Sigrist, The intriguing superconductivity of strontium ruthenate, Phys. Today **54**(1), 42 (2001).

[7] A. P. Mackenzie and Y. Maeno, The superconductivity of Sr_2RuO_4 and the physics of spin-triplet pairing, Rev. Mod. Phys. **75**, 657 (2003).

[8] J. Jang, D. G. Ferguson, V. Vakaryuk, R. Budakian, S. B. Chung, P. M. Goldbart, and Y. Maeno, Observation of half-height magnetization steps in Sr_2RuO_4, Science **331**, 186 (2011).

[9] Y. Maeno, S. Kittaka, T. Nomura, S. Yonezawa, and K. Ishida, Evaluation of spin-triplet superconductivity in Sr_2RuO_4, J. Phys. Soc. Jpn. **81**, 011009 (2012).

[10] C. Kallin, Chiral p-wave order in Sr_2RuO_4, Rep. Prog. Phys. **75**, 042501 (2012).

[11] A. P. Mackenzie, T. Scaffidi, C. W. Hicks, and Y. Maeno, Even odder after twenty-three years: The superconducting order parameter puzzle of Sr_2RuO_4, npj Quantum Mater. **2**, 40 (2017).

[12] S. Ran, C. Eckberg, Q.-P. Ding, Y. Furukawa, T. Metz, S. R. Saha, I.-L. Liu, M. Zic, H. Kim, J. Paglione, and N. P. Butch, Nearly ferromagnetic spin-triplet superconductivity, Science **365**, 684 (2019).

[13] Y. Li, X. Xu, M.-H. Lee, M.-W. Chu, and C. L. Chien, Observation of half-quantum flux in the unconventional superconductor β-Bi_2Pd, Science **366**, 238 (2019).

[14] X. Xu, Y. Li, and C. L. Chien, Spin-Triplet Pairing State Evidenced by Half-Quantum Flux in a Noncentrosymmetric Superconductor, Phys. Rev. Lett. **124**, 167001 (2020).

[15] D. Aoki, J.-P. Brison, J. Flouquet, K. Ishida, G. Knebel, Y. Tokunaga, and Y. Yanase, Unconventional superconductivity in UTe_2, J. Phys.: Condens. Matter **34**, 243002 (2022).

[16] L. Fu and C. L. Kane, Superconducting Proximity Effect and Majorana Fermions at the Surface of a Topological Insulator, Phys. Rev. Lett. **100**, 096407 (2008).

[17] Z. Wang, P. Zhang, G. Xu, L. K. Zeng, H. Miao, X. Xu, T. Qian, H. Weng, P. Richard, A. V. Fedorov, H. Ding, X. Dai, and Z. Fang, Topological nature of the $FeSe_{0.5}Te_{0.5}$ superconductor, Phys. Rev. B **92**, 115119 (2015).

[18] X. Wu, S. Qin, Y. Liang, H. Fan, and J. Hu, Topological characters in $Fe(Te_{1-x}Se_x)$ thin films, Phys. Rev. B **93**, 115129 (2016).

[19] G. Xu, B. Lian, P. Tang, X.-L. Qi, and S.-C. Zhang, Topological Superconductivity on the Surface of Fe-Based Superconductors, Phys. Rev. Lett. **117**, 047001 (2016).

[20] P. Zhang, K. Yaji, T. Hashimoto, Y. Ota, T. Kondo, K. Okazaki, Z. Wang, J. Wen, G. D. Gu, H. Ding, and S. Shin, Observation of topological superconductivity on the surface of an iron-based superconductor, Science **360**, 182 (2018).

[21] T. Machida, Y. Sun, S. Pyon, S. Takeda, Y. Kohsaka, T. Hanaguri, T. Sasagawa, and T. Tamegai, Zero-energy vortex bound state in the superconducting topological surface state of Fe(Se,Te), Nat. Mater. **18**, 811 (2019).

[22] W. A. Little and R. D. Parks, Observation of Quantum Periodicity in the Transition Temperature of a Superconducting Cylinder, Phys. Rev. Lett. **9**, 9 (1962).

[23] F. Loder, A. P. Kampf, T. Kopp, J. Mannhart, C. W. Schneider, and Y. S. Barash, Magnetic flux periodicity of h/e in superconducting loops, Nat. Phys. **4**, 112 (2008).

[24] V. Juričić, I. F. Herbut, and Z. Tesanovic, Restoration of the Magnetic hc/e-Periodicity in Unconventional Superconductors, Phys. Rev. Lett. **100**, 187006 (2008).

[25] J.-X. Zhu and H. T. Quan, Magnetic flux periodicity in a hollow d-wave superconducting cylinder, Phys. Rev. B **81**, 054521 (2010).

[26] V. B. Geshkenbein, A. I. Larkin, and A. Barone, Vortices with half magnetic flux quanta in heavy-fermion superconductors, Phys. Rev. B **36**, 235 (1987).

[27] J. Ge, P. Wang, Y. Xing, Q. Yin, H. Lei, Z. Wang, and J. Wang, Discovery of charge-4e and charge-6e superconductivity in kagome superconductor CsV_3Sb_5, arXiv:2201.10352 (2022).

[28] G. B. Halász, Fractional magnetoresistance oscillations in spin-triplet superconducting rings, arXiv:2111.09333 (2021).

[29] L.-F. Zhang, Z. Wang, and X. Hu, Higgs-Leggett mechanism for the elusive 6e superconductivity observed in kagome vanadium-based superconductors, arXiv:2205.08732.

[30] Z. Pan, C. Lu, F. Yang, and C. Wu, Frustrated superconductivity and "charge-6e" ordering, arXiv:2209.13745 (2022).

[31] V. Vakaryuk and V. Vinokur, Effect of Half-Quantum Vortices on Magnetoresistance of Perforated Superconducting Films, Phys. Rev. Lett. **107**, 037003 (2011).

[32] Y. Yasui, K. Lahabi, M. S. Anwar, Y. Nakamura, S. Yonezawa, T. Terashima, J. Aarts, and Y. Maeno, Little-Parks oscillations with half-quantum fluxoid features in Sr_2RuO_4 microrings, Phys. Rev. B **96**, 180507(R) (2017).

[33] X. Cai, B. M. Zakrzewski, Y. A. Ying, H.-Y. Kee, M. Sigrist, J. E. Ortmann, W. Sun, Z. Mao, and Y. Liu, Magnetoresistance oscillation study of the spin counterflow half-quantum vortex in doubly connected mesoscopic superconducting cylinders of Sr_2RuO_4, Phys. Rev. B **105**, 224510 (2022).

[34] I. Sochnikov, A. Shaulov, Y. Yeshurun, G. Logvenov, and I. Božović, Large oscillations of the magnetoresistance in nanopatterned high-temperature superconducting films, Nat. Nanotechnol. **5**, 516 (2010).

[35] I. Sochnikov, A. Shaulov, Y. Yeshurun, G. Logvenov, and I. Božović, Oscillatory magnetoresistance in nanopatterned superconducting $La_{1.84}Sr_{0.16}CuO_4$ films, Phys. Rev. B **82**, 094513 (2010).

[36] X. Cai, Y. A. Ying, N. E. Staley, Y. Xin, D. Fobes, T. J. Liu, Z. Q. Mao, and Y. Liu, Unconventional quantum oscillations in mesoscopic rings of spin-triplet superconductor Sr_2RuO_4, Phys. Rev. B **87**, 081104(R) (2013).

[37] S. A. Mills, C. Shen, Z. Xu, and Y. Liu, Vortex crossing and trapping in doubly connected mesoscopic loops of a single-crystal type-II superconductor, Phys. Rev. B **92**, 144502 (2015).

[38] K. Aoyama, Little-Parks oscillation and d-vector texture in spin-triplet superconducting rings with bias current, Phys. Rev. B **106**, L060502 (2022).

[39] We assume that spin-orbit coupling forces the Cooper pair d-vector into the plane perpendicular to the spin quantization axis. For a sufficiently high-symmetry layered material, specific mechanisms producing such spin-orbit coupling are described in Ref. [9].

[40] K. Machida and R. Klemm, Incomplete Meissner effect of triplet superconductivity, Solid State Commun. **27**, 1061 (1978).

[41] D. E. McCumber and B. I. Halperin, Time scale of intrinsic resistive fluctuations in thin superconducting wires, Phys. Rev. B **1**, 1054 (1970).

[42] Y. S. Erin, S. V. Kuplevakhski, and A. N. Omelyanchuk, Little-Parks effect for two-band superconductors, Low Temp. Phys. **34**, 891 (2008).

[43] B. I. Halperin, G. Refael, and E. Demler, Resistance in superconductor, in *BCS: 50 Years* (World Scientific, Singapore, 2010), pp. 185–226.

[44] Since the resistance decreases if the critical temperature is increased, it is not surprising that a two-peak structure in the resistance translates into a *two-valley* structure in the critical temperature.

[45] S. B. Chung, H. Bluhm, and E.-A. Kim, Stability of Half-Quantum Vortices in $p_x + ip_y$ Superconductors, Phys. Rev. Lett. **99**, 197002 (2007).

[46] A. Leggett, Inequalities, instabilities, and renormalization in metals and other Fermi liquids, Ann. Phys. **46**, 76 (1968).

[47] A. J. Leggett, A theoretical description of the new phases of liquid ^{3}He, Rev. Mod. Phys. **47**, 331 (1975).